SUPPLEMENTAL DATA

Supplementary Tables and Figures

Supplementary Table 1.

Data base	Pathway	Genes	*P*-Value	FDR
KEGG	ErbB	CDKN1A, PAK2, PLCG1, ERBB3, CAMK2G, ABL2	0.0209	21.2063
KEGG	p53	BID, CDKN1A, CD82, LRDD, BAI1	0.0351	33.1772
Biocarta	Glycolysis	GPI, ALDOB, GAPDH	0.0423	37.5070
KEGG	SNARE	STX6, VAMP1, GOSR1, VAMP4, STX2	0.019134	35.7173

Supplemental Table 1. Gene array analysis in ATP11B-silenced A2780-CP20 cells. The signaling pathways ErbB, p53, Glycolysis and the SNARE (soluble *N*-ethylmaleimide-sensitive-factor attachment protein receptor) were significantly deregulated in ATP11B-silenced A2780-CP20 cells. Integrated function and pathway analysis were performed using DAVID bioinformatics resources (http://david.abcc.ncifcrf.gov/) and significant features were clustered.

Supplementary Table 2

SNARE- genes	ATP11B-siRNA/Cr-siRNA Fold-change	*P*- value
STX6	0.61	0.0040
VAMP1	0.80	0.0045
GOSR1	0.79	0.0478
VAMP4	1.24	0.0260
STX2	1.30	0.0283

Supplementary Table 2. Gene array analysis in ATP11B-silenced A2780-CP20 cells. In ATP11B-silenced A2780-CP20 ovarian cancer cells, five genes of the SNARE pathway were significantly deregulated: syntaxin-4 and 6 (STX4, STX6), vesicle associated membrane protein 1 and 4 (VAMP1 and VAMP4) and Golgi SNAP (synaptosomal associated protein) receptor 1 (GOSR1).

Supplementary Figure 1.

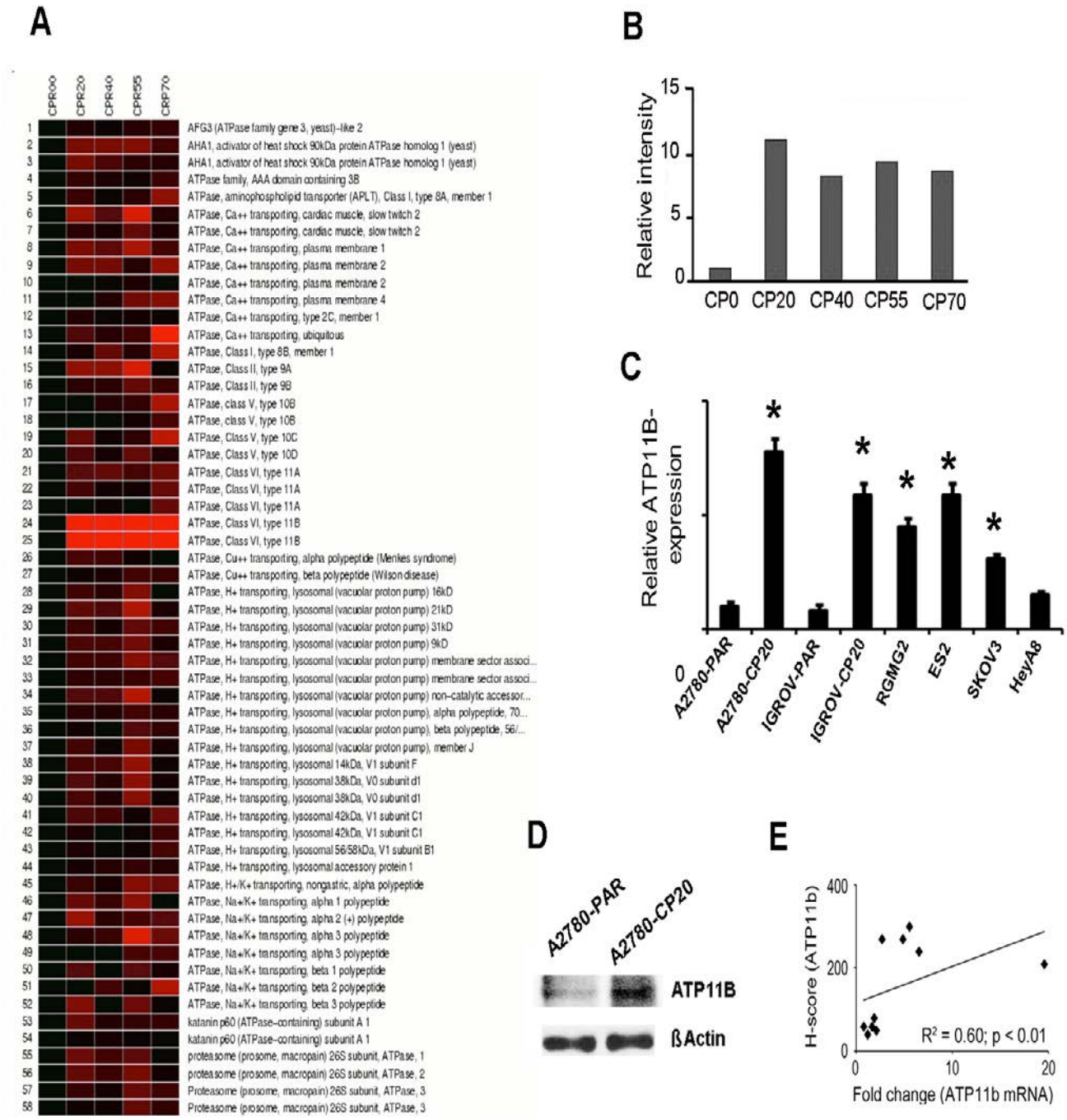

Supplementary Figure 2.

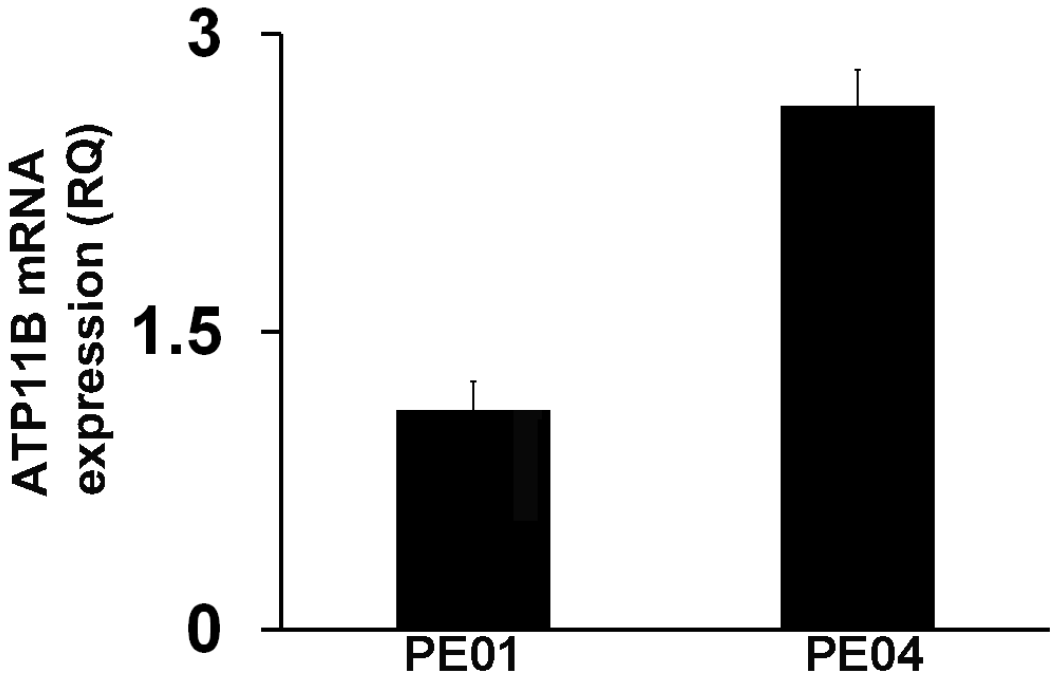

Supplementary Figure 3.

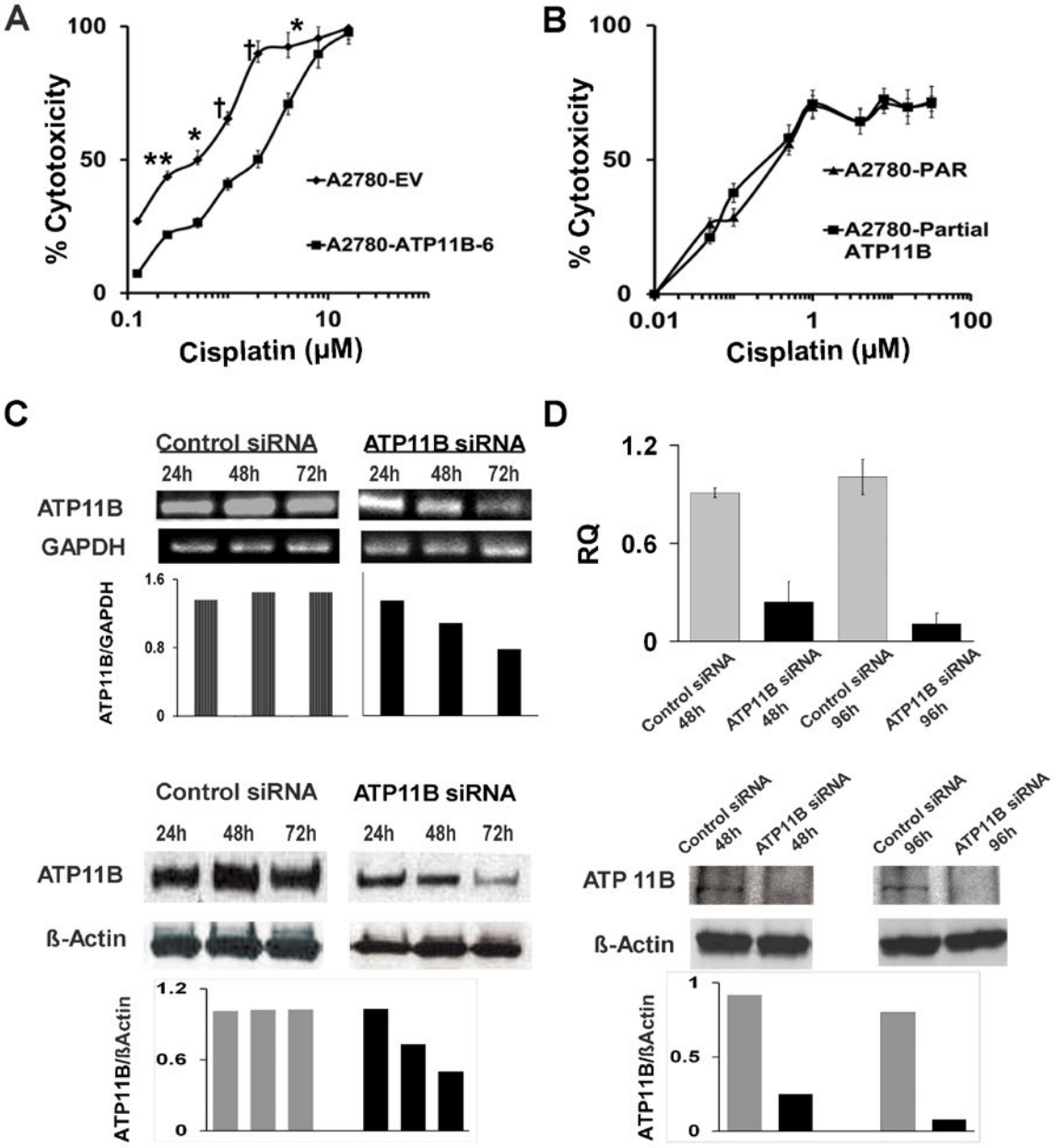

Supplementary Figure 4.

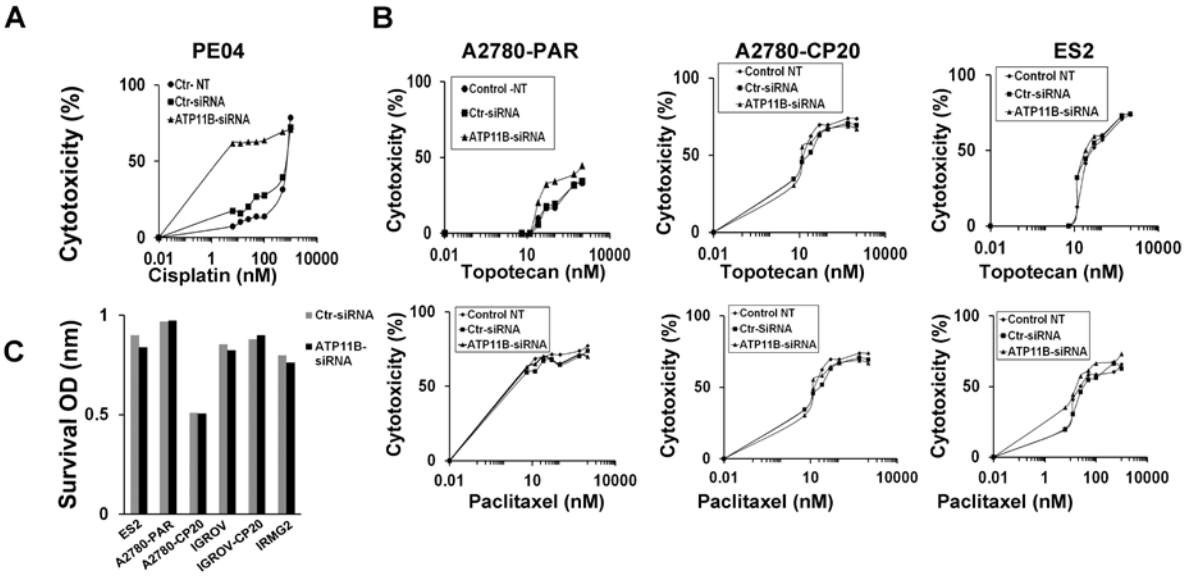

Supplementary Figure 5.

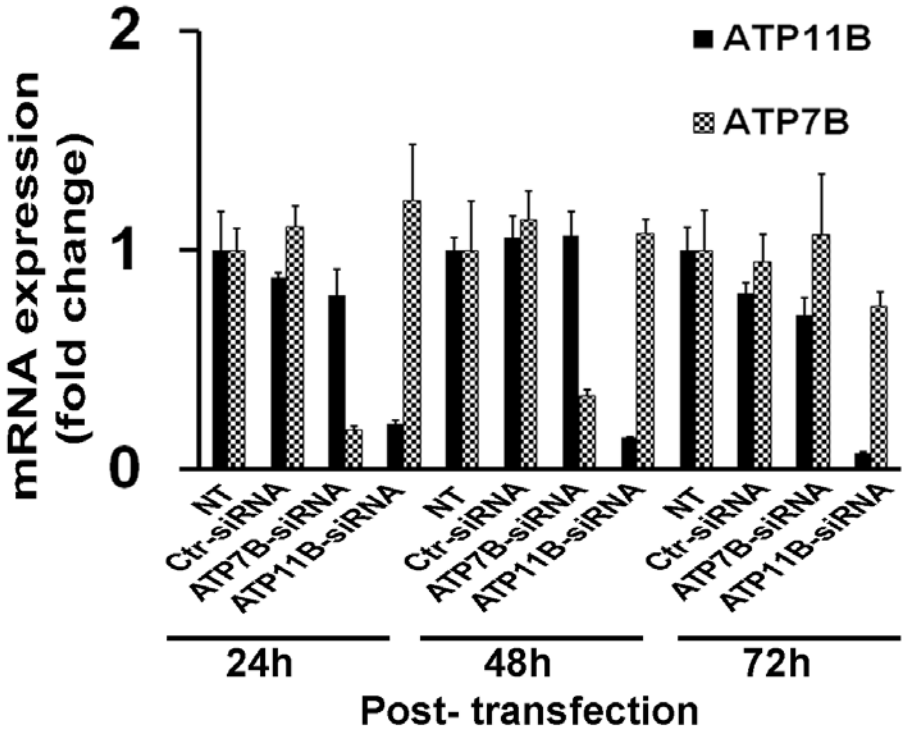

Supplementary Figure 6.

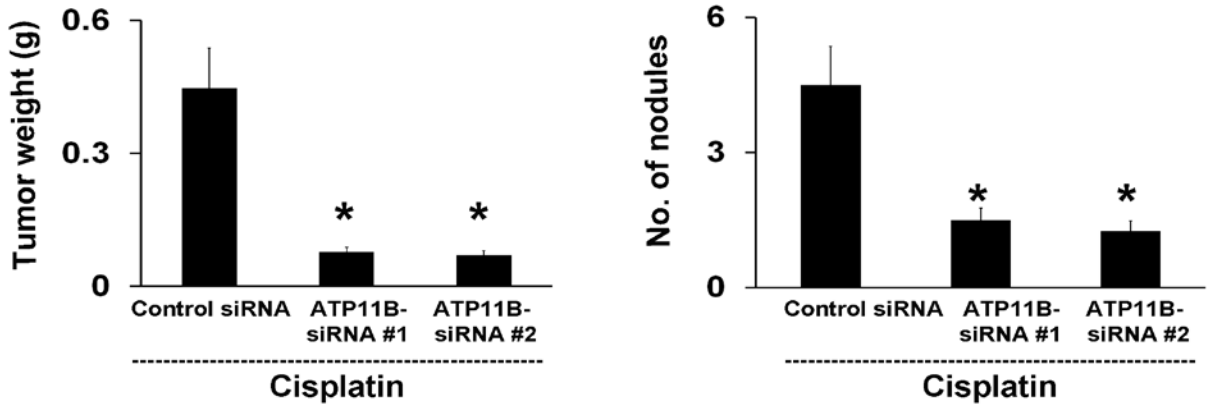

Supplementary Figure 7.

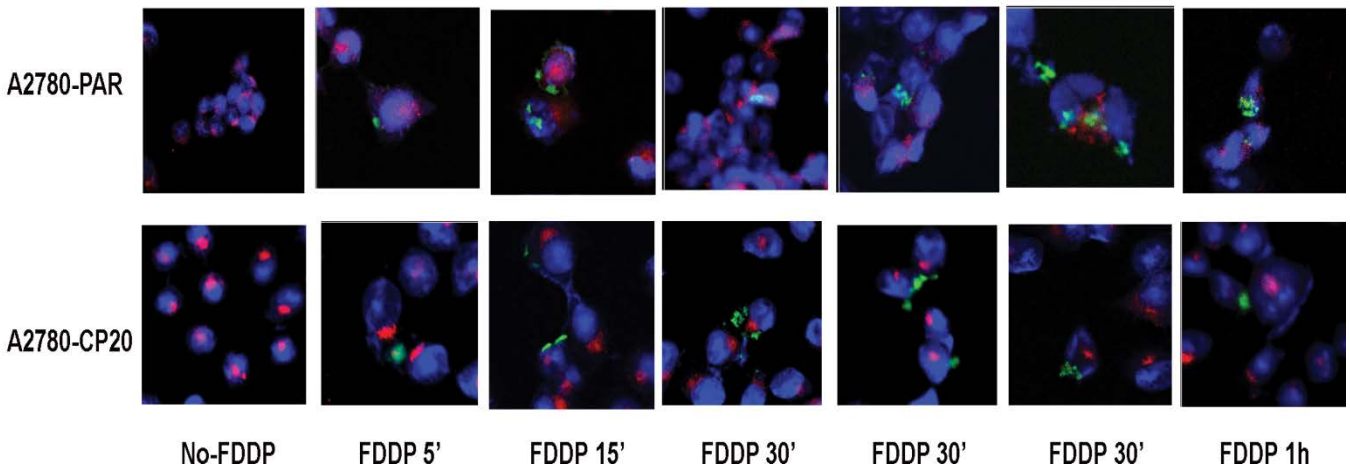

Supplementary Figure 8.

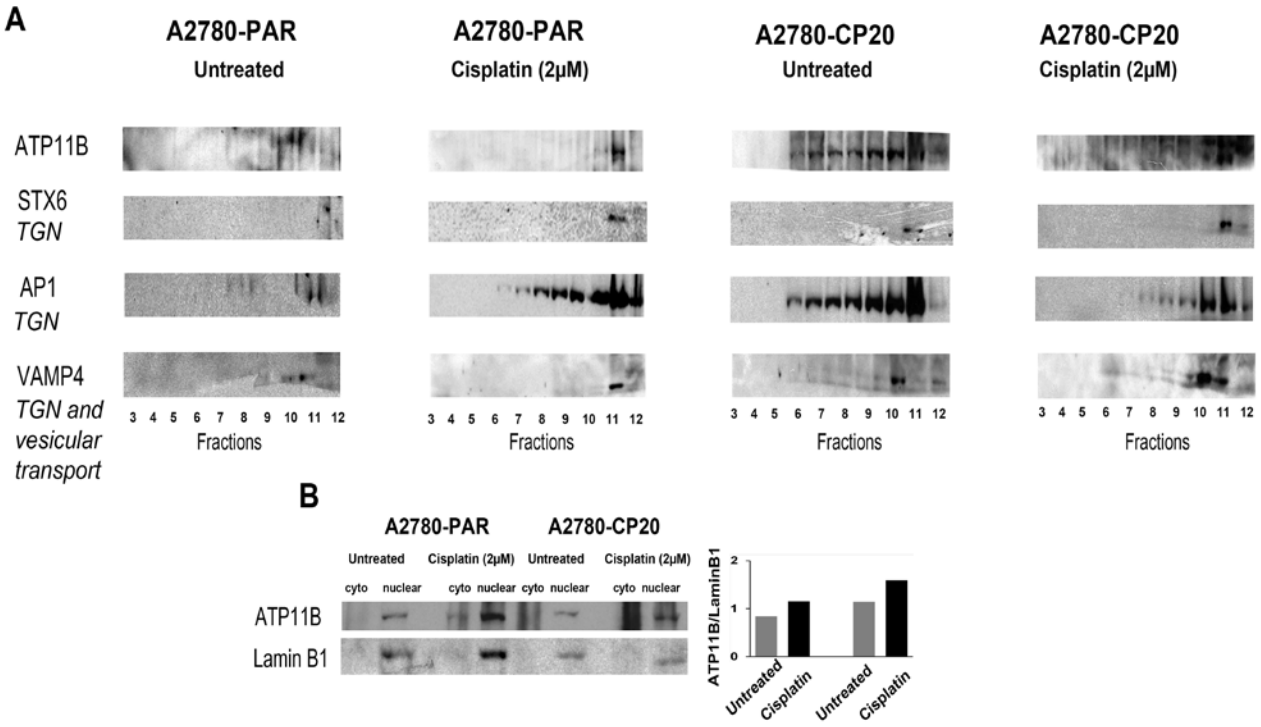

Supplementary Figure 9.

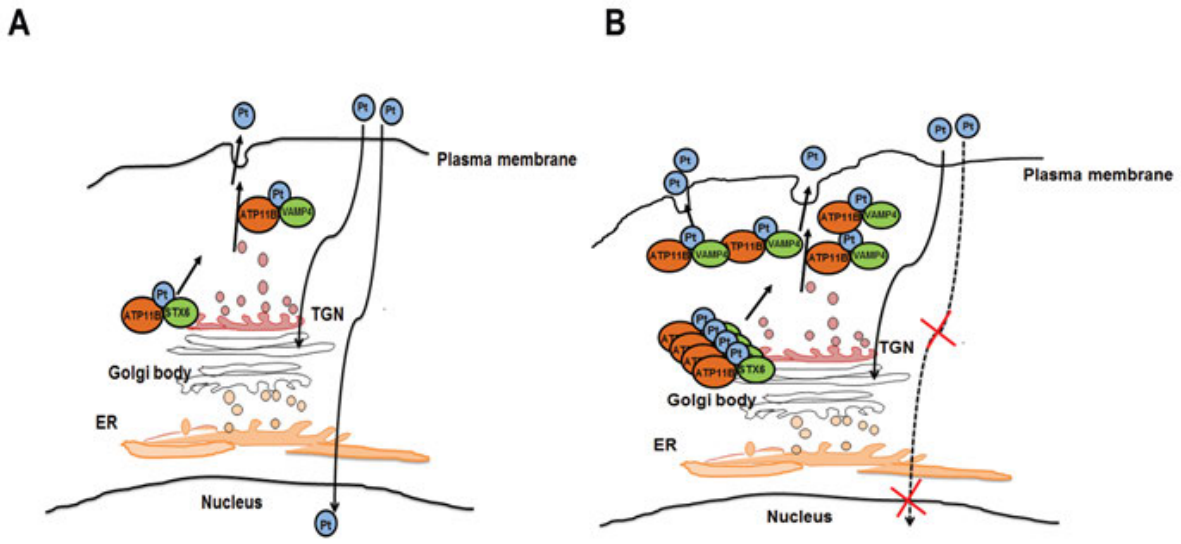

Supplementary Figure 10.

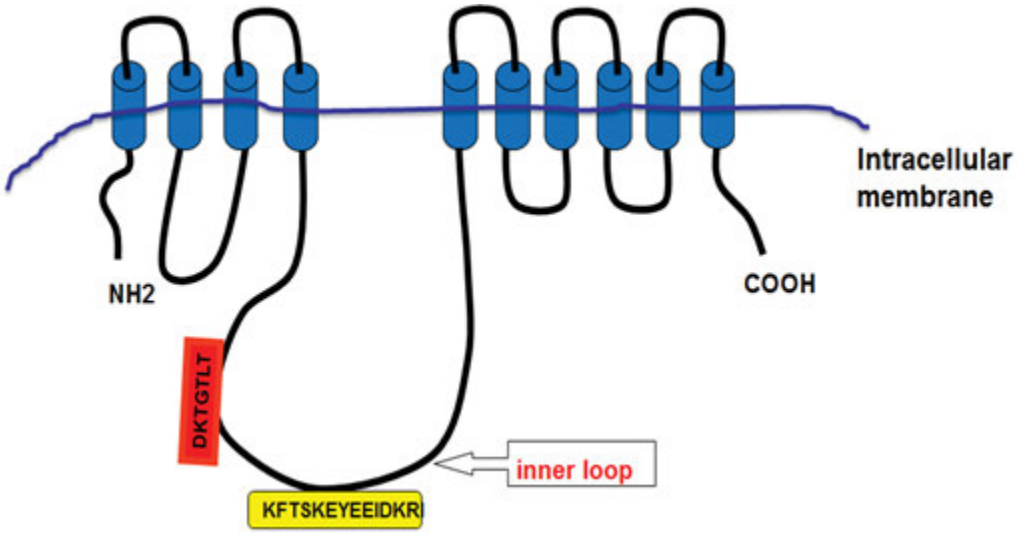

Legends of Supplementary Figures

Supplementary Figure 1

(A) Gene array analyses in human cisplatin-resistant ovarian cancer cells. Heat map showing gene expression profile from ATP-ases in the progressively resistant ovarian cancer cell lines A2780-CP20, CP40, CP55, and CP70, compared with the A2780-PAR cells. ATP11B, a type 4 P-type ATPase transport membrane protein, was highly upregulated in all cell lines tested. **(B)** A2780-CP20 cells had the highest ATP11B expression. **(C)** ATP11B gene expression was also significantly elevated in other cisplatin-resistant ovarian cancer cells (A2780-CP20, IGROV1-CP20, RMG2 ,ES2), and SKOV3, compared with the highly sensitive A2780-PAR cells (*$P < 0.01$). **(D)** Protein expression was confirmed to be increased in the A2780-CP20 cells compared with the A2780-PAR cells. **(E)** Significant correlation between ATP11B mRNA and protein expression.

Supplementary Figure 2

ATP11B mRNA expression in primary human ovarian cancer cells P0E1 and P0E4 cells. Relative quantification (RQ) values were normalized to a house keeping gene (18S) and then normalized to a calibrator sample (normal ovarian tissue) according to the 2-ΔΔCt comparative threshold cycle (Ct) method {Livak, 2001 #19854} TD). P0E4 (chemo-resistant) cells exhibited 2.4 fold greater ATP11B expression levels compared to those from P0E1 (chemo-sensitive) cells. A value of RQ 1 was assigned to P0E1 cells.

Supplementary Figure 3

(A) Half-maximal inhibitory concentration (IC_{50}) was determined by means of the MTT assay using a wide range of cisplatin concentrations (0-32 μM). IC_{50} for A2780-EV and A2780-ATP11B-6 were 0.52 and 2.0 μM, respectively (*P < 0.05; **P < 0.01; †P < 0.001). **(B)** In contrast, the IC_{50} of A2780 cells transfected with C-terminal partial ATP11B sequence was very similar to the IC_{50} for A2780 parental cells. **(C)** RT-PCR analysis of ATP11B expression in A2780-PAR cells transfected with control-siRNA and with ATP11B-siRNA. Compared with control-siRNA transfected cells, ATP11B mRNA expression was decreased by >50% in the ATP11B-siRNA transfected cells. Western blotting analyses confirmed the decrease of ATP11B protein expression (29 and 52%) after the same transfection times (48 and 72 hours). **(D)** mRNA expression of ATP11B in A2780-CP20 tumor tissues harvested at 48 and 98 hours after injection of a single dose of ATP11B siRNA-DOPC (150 μg/kg i.p.). QRT-PCR data indicated a decrease in ATP11B expression levels of 74 and 89% after 48 and 96 hours, respectively, compared to those from tumor tissues injected with Ctr-siRNA. ATP11B protein levels were similarly reduced (73 and 90%) after 48 and 96 hours of ATP11B siRNA-cell injection.

Supplementary Figure 4

(A) ATP11B downregulation increases sensitivity of primary ovarian cancer (chemo-resistant) P0E4 cells to cisplatin (*P < 0.05). **(B)** Survival curves from primary ovarian cancer cells: A2780-PAR, A2780-CP20 and ES2 showing no significant effect of ATP11B silencing on sensitivity to paclitaxel or topotecan. **(C)** ATP11B silencing did not significantly affect survival of ovarian cancer cells: ES2, A2780-PAR, A2780-CP20, IGROV, IGROV-CP20 and RMG2.

Supplementary Figure 5

ATP7A and ATP11B expression levels are not coordinately regulated in A2780-CP20 cells. QPCR analysis showed no significant change in ATP7B levels following ATP11B gene silencing; similarly no significant changes in ATP11B levels were noted following ATP7B gene silencing compared with their corresponding Ctr-siRNA or not-treated (NT) A2780-CP20 cells.

Supplementary Figure 6

Effect of two independent ATP11B-siRNA sequences in combination with cisplatin on A2780-CP20 tumor growth. Treatments of ATP11B-siRNA-DOPC (Seq. #1) or ATP11B-siRNA-DOPC (Seq. #2) plus cisplatin significantly blocked tumor growth (83, 85%: ***P** < 0.05) and reduced the number of tumor nodules (67, 72%; ***P** < 0.05), respectively, compared to Ctr-siRNA mice group. Data are means ± SE. N=5 mice/group.

Supplementary Figure 7

Immunofluorescence confocal images (200×) from 2780-PAR and A2780-CP20 cells in the presence of fluorescent cisplatin (FDDP). A2780-PAR and A2780-CP20 cells were exposed to 2 μM green FDDP for different times (5 minutes up to 1 hour) and immunostained for detection of ATP11B. After 30 minutes and 1 hour of FDDP exposure, FDDP was frequently detected in the nucleus of A2780-PAR cells. In contrast, FDDP was seldom found in the nucleus of A2780-CP20 cells (green: FDDP; red: ATP11B; blue: nuclei).

Supplementary Figure 8

Distribution of ATP11B and SNARE proteins in sucrose gradient fractions. **(A)** Endomembrane fractions were prepared from A2780-PAR and A2780-CP20 cells, untreated and cisplatin-treated. After sucrose-gradient fractionation, an equal-volume samples from each gradient fraction were separated by SDS-PAGE and probed by Western blotting against a panel of Golgi and endosomal protein markers. The main subcellular localization of each protein is shown in italics. **(B)** ATP11B localization was analyzed in cytosolic and nuclear fractions from these cells. Lamin B1 was used as a nuclear protein marker.

Supplementary Figure 9

Hypothetical model of the role of ATP11B in platinum transport in ovarian cancer cells. **(A)** Inside cisplatin-sensitive cells, the trans-golgi-network (TGN) is one of the main Pt-target compartments. In the TGN, Pt may be temporarily sequestered and/or may be captured in TGN-intermediate/ secretory vesicles for export. ATP11B and the SNARE proteins: syntaxin 6 (STX6) and vesicular associated membrane protein 4 (VAMP4) enhance Pt efflux via the vesicular secretory pathway. Pt also targets its ultimate cellular target, the nuclear DNA**. (B)** In cisplatin-resistant cells, upregulation of ATP11B increases vesicular-mediated-Pt export, preventing Pt from reaching the nucleus.

Supplementary Figure 10

ATP11B is a Type 4 P-type ATPase-transport membrane protein. The protein structure of ATP11B shows ten transmembrane (TM) domains. P-type ATPase phosphorylation consensus sequence (red box) is located in TM4. The sequence at the inner loop from TM4 (yellow box) was used to raise a rabbit antiserum (Sigma) against ATPB11-protein.